JOURNAL OF MATERIALS SCIENCE **35** (2000) 2779–2784

High-strain-rate superplastic deformation behavior of a powder metallurgy-processed 2124 Al alloy

W. J. KIM
Department of Metallurgy and Materials Science, Hong-Ik University, 72-1 Sangsung-dong, Mapo-ku, Seoul, South Korea
E-mail: kimwj@wow.hongik.ac.kr

S. H. HONG
Department of Materials Science and Engineering, Korea Advanced Institute of Science and Technology, 373-1 Kusung-dong, Yususng-gu, South Taejon 305-701, South Korea

High-strain-rate superplastic behavior of a powder-metallurgy processed 2124 alloy prepared through extrusion at a high ratio of 70 : 1 was investigated. A maximum tensile elongation of 700% was obtained at 823 K and at a strain rate of 10^{-2} s^{-1}. Deformation behavior of this alloy was similar to those reported for other many HSR superplastic materials. Incorporation of threshold stress into the constitutive equation reveals that the true stress exponent is 2 and true activation energy for plastic flow is comparable to that for lattice diffusion in pure aluminum. Comparison of the present alloy with the 2124 Al composite indicates that the composite is weaker than the unreinforced alloy in the temperature range where grain boundary sliding is rate-controlled.

1. Introduction

High-Strain-Rate Superplasticity (hereafter, HSRS), meaning high tensile elongation at high strain rates, in several classes of materials including alloys, metal matrix composites (MMCs) and mechanically-alloyed materials has been realized through recent advance in power-metallurgy technology [1–16]. Among the many HSR superplastic MMCs, 2124 Al composites reinforced by either SiC_w, Si_3N_{4p} or Si_3N_{4w} have been most extensively studied to data [1, 2, 6, 16] since Nieh *et al*. [1] witnessed a HSRS phenomenon in a powder-metallurgy (PM) processed 20%SiC_w/2124 Al composite. HSR superplastic flow characteristics of an unreinforced PM 2124 Al alloy that is the very matrix alloy for the PM 2124 Al composites, however, has been never studied in detail. The present research is to evaluate superplastic proprieties of a PM 2124 Al alloy at elevated temperatures. These data are believed to be particularly valuable helping to understand the deformation behavior of HSR superplastic 2124 composites that are currently in debate [17–19].

2. Experimental methods

The material used in the current investigation was prepared by powder-metallurgy routes. Commercial 2124 Al powders were supplied by Changsung Ltd. The Al powders with an average size of 20 μm were cleaned ultrasonically in an alcoholic solvent and then dried in air. The mixed powders were consolidated at 843 K in a vacuum hot press with a pressure of 90 MPa for 0.2 hr. The consolidated billet was then extruded by 70 : 1 at a temperature of 723 K. Tensile test samples with a gage length of 6 mm were machined from the extruded bar with tensile axis parallel to the extrusion direction. Strain-rate-change (SRC) tests were conducted in air at temperatures between 643 K and 823 K and at strain rates between 10^{-4} s^{-1} and 10^{-1} s^{-1} to evaluate the strain rate-stress relationship. Elongation-to-failure tests were carried out under constant cross-under constant cross-head speed condition. The microstructures of the samples were investigated by optics and transmission electron microscope (TEM).

3. Experimental results and discussion

Fig. 1a shows a photograph showing a typical microstructure of the 2124 Al alloy obtained after extrusion. The grains are equiaxed and fine, and have an average size of 3.2 μm. A TEM micrograph of the same alloy is shown in Fig. 1b. Low angle boundaries were often encountered during TEM observation. Precipitates such as Al_2Cu and Al_2CuMg are uniformly distributed over the matrix. The result of elongation-to-failure tests performed at several temperatures and strain rates is provided in Fig. 2. Superplastic temperature range was found between 773 and 823 K, where tensile elongations over 300% could be achieved. Tensile elongation shows the tendency to increase with increasing temperature but decreases abruptly beyond 823 K. The largest

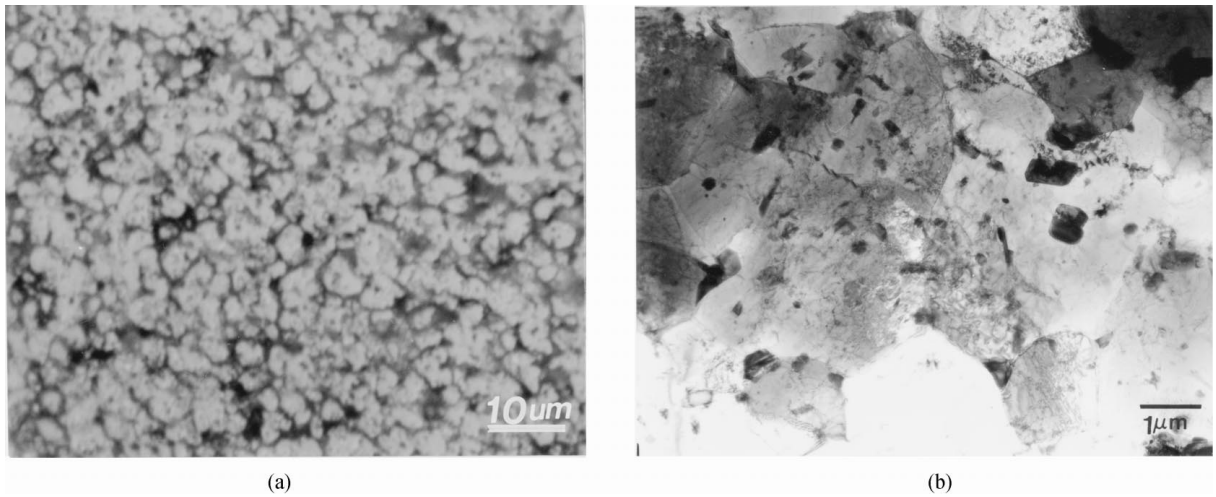

Figure 1 (a) A photograph of the PM 2124 Al alloy after extrusion (b) A TEM micrograph of the same material.

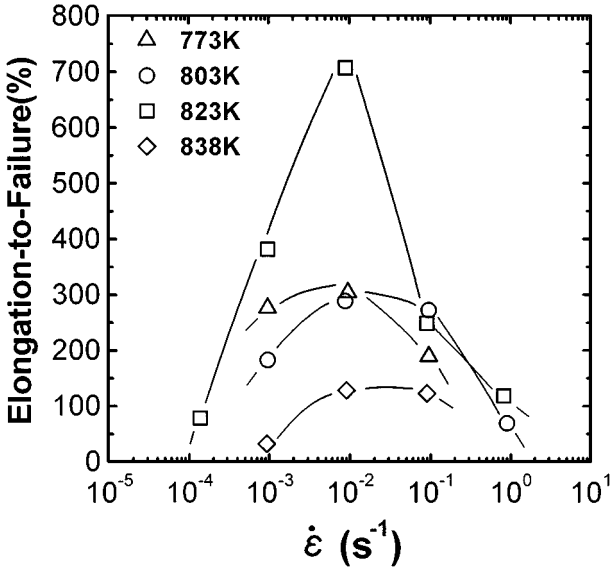

Figure 2 The result of elongation-to-failure tests conducted at various temperatures and strain rates.

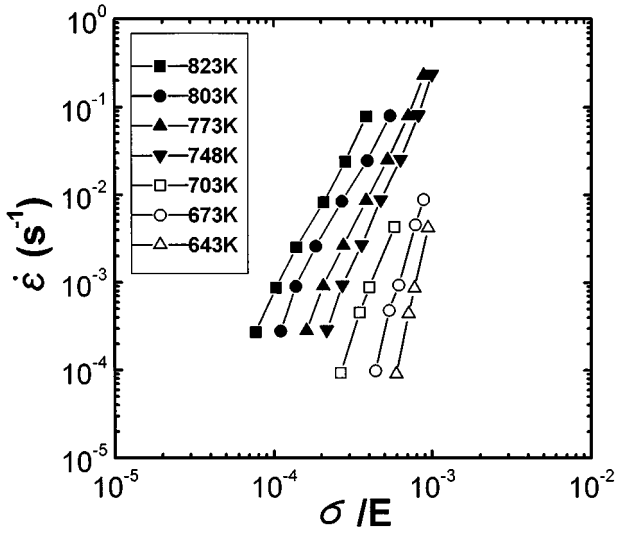

Figure 3 Strain rate-flow vs. stress relationship for the PM 2124 alloy in a temperature range between 643 K and 823 K.

tensile elongation of 700% was obtained at 823 K. This optimum temperature for superplasticity is significantly higher than the solidus temperature of the 2124 Al alloy, known as 780 K [20]. Achievement of HSRS near or above the solidus temperature is a common phenomenon found in many HSR superplastic materials [4, 17]. The reason may be due to the introduction of some liquid phase acting as lubricants to promote grain boundary sliding or relive stress concentration causing cavitation, allowing superplastic flow to occur at very high strain rates. The strain rate effect on tensile elongation is as follows at the optimum temperature of 823 K. A tensile elongation was as small as 70% at a low strain rate of 10^{-4} s^{-1}. But it increased rapidly with increasing strain rate and reached the maximum value of 700% at 10^{-2} s^{-1}. Beyond the strain rate of 10^{-2} s^{-1}, it dropped quickly but the material yet exhibited good superplasticity, with elongation staying 300% up to 10^{-1} s^{-1}. The rapid decrease in total elongation beyond 823 K, on the other hand, seems due to the presence of excessive liquid phase.

Fig. 3 shows the relationship between strain rate and modulus-compensated stress in a log-log plot at various temperatures between 643 and 823 K. At the temperature interval between 748 and 823 K, the slope of the curve, representing the value of apparent stress exponent, n_a, varies with strain rate. A gradual decrease in n_a value with increasing strain rate is followed by a jump in the high strain rate range, in a typical sigmodal curve as has been observed for many superplastic metallic alloys. The similar trend of decreasing n_a with increasing strain rate is also observable in the lower temperature range between 647 and 703 K, but with the measured n_a values are larger. Fig. 4 shows the relationship between the apparent strain-rate-sensitivity exponent, $m_a(=1/n_a)$, measured from the slope for the strain rate-stress curve at 823 K and total elongation-to-failure (%) as a function of strain rate. As can be seen, high elongations are obtained at the strain rate range coinciding with the range where high values of m_a were measured.

In the following analysis, the presence of threshold stress is assumed to be responsible for the display of curvature in the strain rate-stress relationship

shown in Fig. 3. If a threshold stress, σ_0, below which deformation does not occur, exists, the deformation of a material is driven by an effective stress, $\sigma - \sigma_0$. In this case, the plastic flow behavior is described by the following equation.

$$\dot{\varepsilon} = AD\left(\frac{b}{d}\right)^p \left(\frac{\sigma - \sigma_0}{E}\right)^n \quad (1)$$

where b the Burgers vector, D the relevant diffusivity, E the Young's modulus, d the grain size, p the grain size exponent, and A a geometrical constant. If the deformation behavior of the present alloy obeys Equation 1, the threshold stress at a given temperature can be determined by selecting a proper n value giving the best linear fit to the datum points in the plot $\dot{\varepsilon}^{1/n}$ vs. σ and then, extrapolating them to the zero strain rate with a linear regression. Fig. 5 shows that the entire temperature range could be divided into two regions from the viewpoint of n value yielding the best linearity: Region I covers the temperature range between 643 and 703 K and Region II does the range between 748 and 823 K. In the current threshold stress analysis, the data for high strain rates in Region II, probably representing normal high temperature creep mechanism(dislocation climb creep) or powder-law breakdown, are not included. The data plotted in Fig. 5 indicates that the n value for the best linearity is equally reasonably good at 2 and 3 in Region I, while it is 5 in Region II. The relations between strain rate and modulus-compensated effective stress obtained by assuming $n = 2$ and $n = 3$, respectively, are presented in Fig. 6a and b. Inspection reveals that except for the data at very high strain rates, most of datum points in Region II fit well to a series of parallel lines having a slope which gives $n = 2$ or 3. The similar result of parallel lines can be observed with $n = 5$ in Region I (Fig. 6c). The deformation mechanisms associated with $n = 2$ and $n = 3$ are most likely to be grain boundary sliding and solute drag creep, respectively, while $n = 5$ corresponds to dislocation climb creep

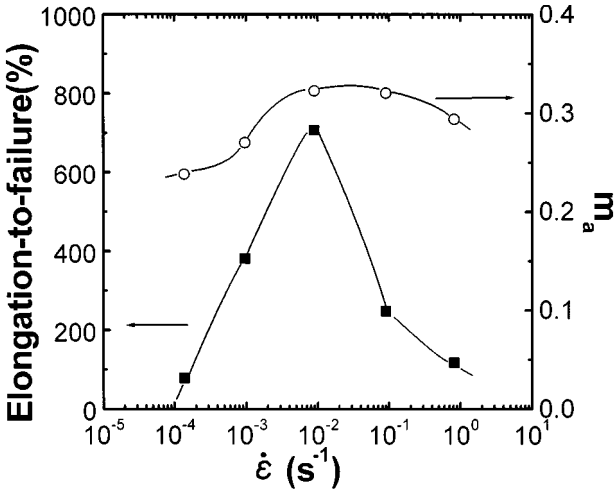

Figure 4 The relationship between m_a and total elongation at 823 K.

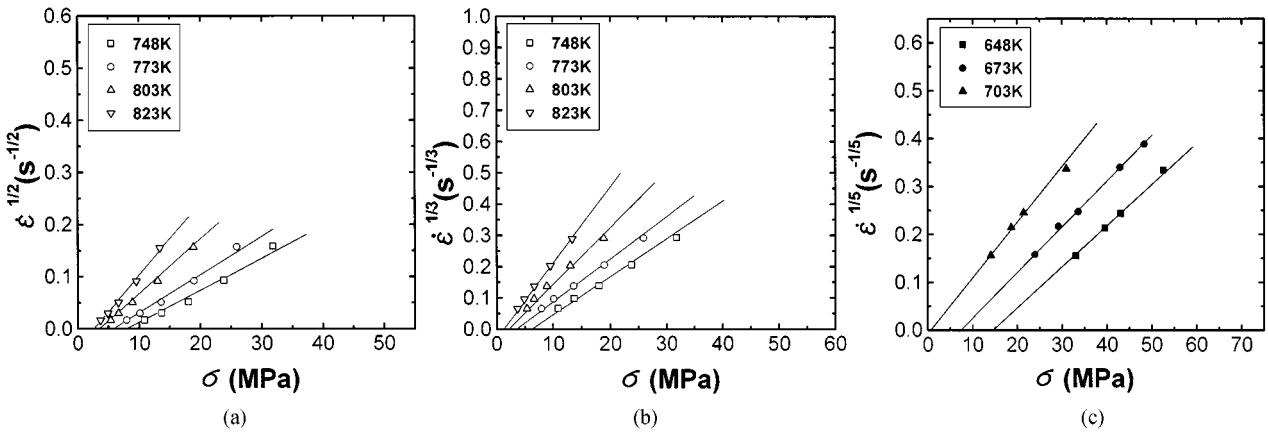

Figure 5 Linear plots of $\dot{\varepsilon}^{1/n}$ vs. σ for the PM 2124 Al alloy using values of n of (*a*) $n = 2$ for Region II (b) $n = 3$ for Region II (c) $n = 5$ for Region I.

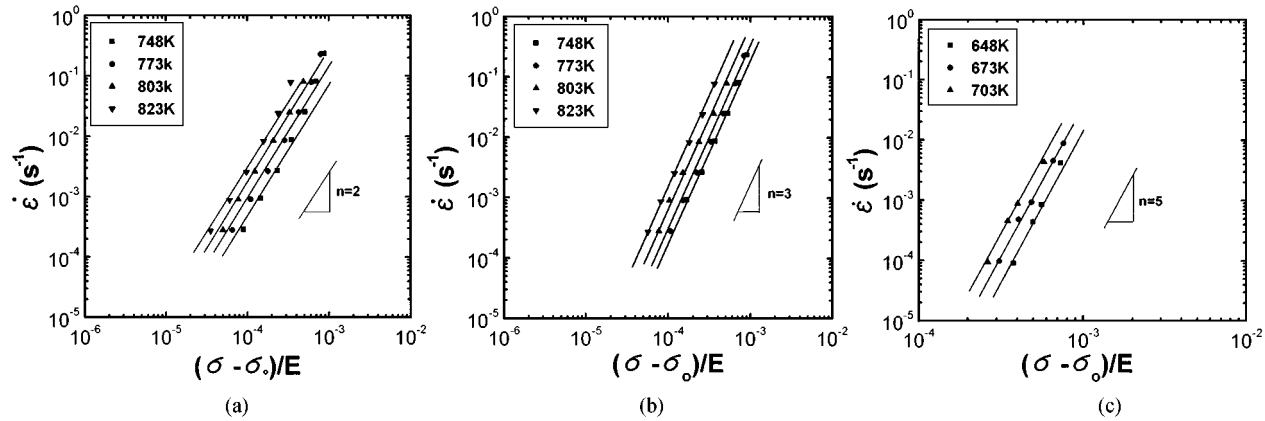

Figure 6 Strain rate vs. modulus-compensated effective stress for the PM 2124 Al alloy (a) $n = 2$ for Region II (b) $n = 3$ for Region II (c) $n = 5$ for Region I.

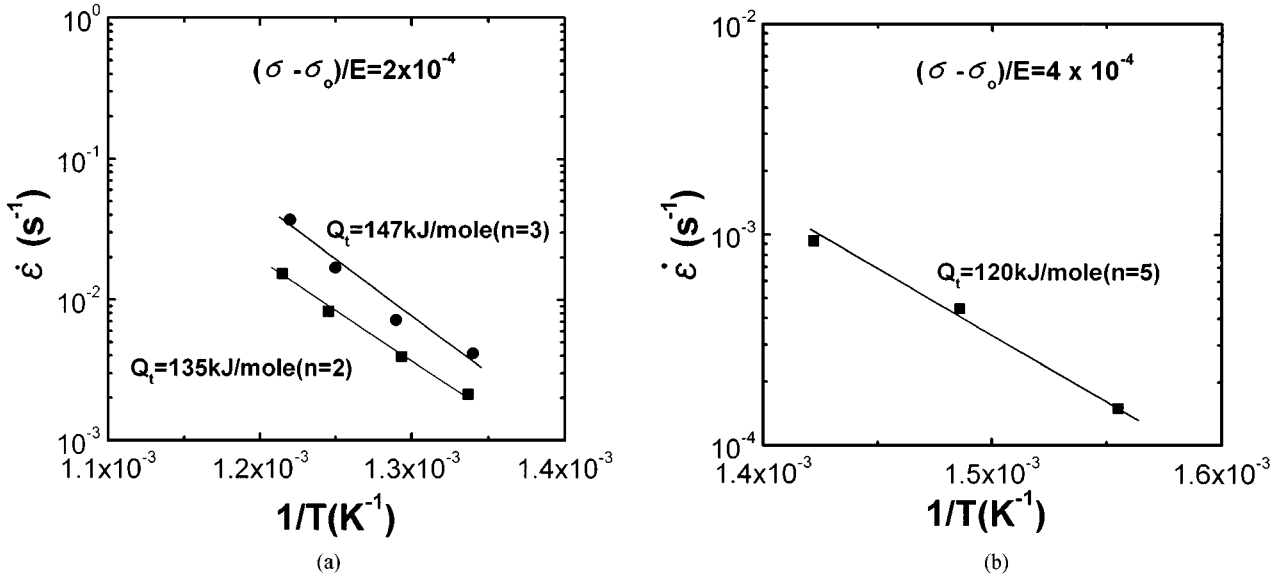

Figure 7 Measurement of true activation energy for the PM 2124 Al alloy.

(lattice diffusion controlled). The threshold stress values measured in Fig. 5 are listed in Table I.

The values of true activation energy, Q_t, for superplastic flow and creep could be estimated from a semilogarithmic plot of $\dot{\varepsilon}$ against $1/T$ at a given modulus-compensated effective stress. This plot is given in Fig. 7. The Q_t values measured in Region II are 135 kJ/mole and 147 kJ/mole for $n = 2$ and for $n = 3$, respectively (Fig. 7a). Both values are very close to the activation energy for self-diffusion in pure Al. It is, therefore, hard to judge from the value of Q_t which mechanism depicts the deformation behavior of the present alloy better. Examination of grain size effect on plastic flow is believed to provide a good guide helping to determine which of the two mechanisms is the rate-controlling process. This is because grain boundary sliding is expected to show a strong grain size dependence on the plastic flow whereas solute drag creep is not. To investigate the grain size effect on plastic flow, the 2124 Al alloy was exposed to 773 K for 12 hours to produce coarser grains. The SRC test on this material conducted at 823 K indicates that the strain rate-stress relationship has noticeably changed upon increase in grain size. The strength was found to be higher than that of the original material in the comparison at a given strain rate. Because of this reason, it is most likely that the rate-controlling deformation process in Region II is grain boundary sliding. The result of $Q_t = Q_L$ observed in Region II is in a good agreement with those for HSR superplastic PM Al-Ti-Fe and 7475 Al+0.7Zr alloys studied recently by Kim *et al.* [14, 15] and many other HSR superplastic alloys [21]. This finding, however, contrasts with the view of Mishira *et al.* [19] and Li and Langdon [18] that the plastic flow of HRS superplastic Al alloy is controlled by grain boundary diffusion. Another point to be noted regarding Q_t in Region II is that the relation of $Q_t = Q_L$ holds even above the solidus temperature. This result implies that the presence of liquid phase does not significantly alter the plastic flow behavior at least up to 823 K. The Q_t valueRegion I (Fig. 7b) is, on the while, 120 kJ/mole. This value is also close to that for self-diffusion in pure aluminum and agrees well with the values reported on the PM 2024 Al alloy [22] and many other aluminum alloys and composites in creep [23–25].

TABLE I The measured threshold stress values for the PM 2124 Al alloy

T (K)	σ_0 ($n=2$)	σ_0 ($n=3$)	σ_0 ($n=5$)
643			12
673			7
703			0.7
748	6.4	5.2	
773	4.7	2.7	
803	2.9	1.6	
823	2	1	

Based on the present analyses, the constitutive equation for the superplastic flow in the present alloy can be written as follows:

$$\dot{\varepsilon} = 3 \times 10^{24} \exp\left(-\frac{135000}{RT}\right)\left(\frac{b}{d}\right)^2\left(\frac{\sigma - \sigma_0}{E}\right)^2 \quad (2)$$

Here, the grain size exponent, p, is assumed to be 2 based on the phenomenological relation developed by Ruano and Sherby [26]. In the present study, the constitutive relation depicting the superplastic flow behavior of a PM 20%Si_3N_{4p}/2124 Al composite [6] (reinforcement and grain sizes are 1 μm and 2 μm respectively) in the temperature range between 758 and 833 K has been analyzed using the similar procedures taken for the PM 2124 Al alloy. The result is

$$\dot{\varepsilon} = 4 \times 10^{58} \exp\left(-\frac{590000}{RT}\right)\left(\frac{b}{d}\right)^2\left(\frac{\sigma - \sigma_0}{E}\right)^2 \quad (3)$$

Comparison of Equations 2 and 3 indicates that the value of A and Q_t are considerably different between the two materials. Mishra *et al.* [19] who analyzed the temperature dependence of the HSR superplastic flow

for several 2124 composites, proposed that the high Q_t may be associated with a contribution from diffusion along the interfaces between the metallic matrices and the ceramic reinforcement. Very recently, Li and Langdon [18] adopted the concept of load transfer depending on temperature to explain the high Q_t, which was originally proposed by Park *et al.* [27] and used in an analysis of the creep of an 6061 Al reinforced by SiC.

The strength between the PM 2124 alloys without and with reinforcement is compared in terms of $(\sigma - \sigma_0)/E$ at a given value of $\dot{\varepsilon}(d/b)^2$ of 10^6. The result is presented as a function of the inverse temperature in Fig. 8. The plot in the figure indicates that the unreinforced alloy is strikingly stronger than the composite, even after the grain-size dependence on plastic flow is compensated and the strength differential between the two alloys increases with increasing temperature. This observation of weaker composite clearly contrasts with that often revealed in creep where strengthening effect by reinforcement is apparent [25, 27]. The opposite trend is, however, expected to be observed at temperatures below 737 K if Equations 2 and 3 continue to hold below this temperature. Conformation of the trend predicted below 737 K can not be provided here because dislocation climb creep shows up as the rate-controlling process from below this temperature (see Fig. 3). Fig. 9 show the plot of $\dot{\varepsilon}(d/b)^2$ vs. σ/E at 773 K constructed by using the data extracted from the strain rate-stress curves for the superplastic ingot-processed 2024 Al alloy [28] and composite [29] reported by Zheng *et al*. The data for the 2024 Al composite in Fig. 9 are those predicted based on the data for 788 K provided by Zheng *et al.* [29] by assuming that lattice diffusion controls the superplastic flow of the composite. Similar result of weaker composite is apparent from the plot. Further studies are required to understand this interesting result of unusual strength differential between the alloys with and without reinforcement.

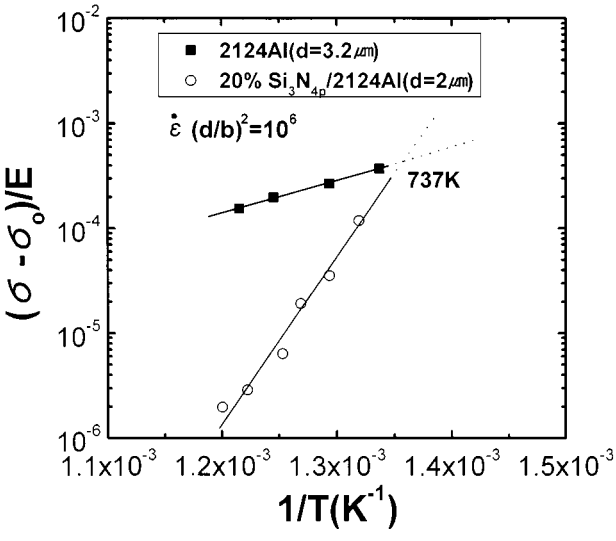

Figure 8 Comparison of modulus-compensated effective stress between the PM 2124 Al alloy and PM 20%Si_3N_{4p}/2124 Al composite at $\dot{\varepsilon}(d/b)^2 = 10^6$.

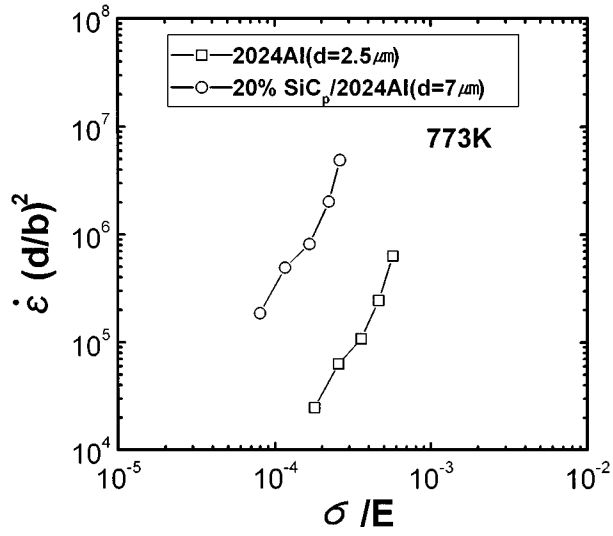

Figure 9 Comparison of strain rate vs. stress relation between ingot-processed superplastic 2024 Al alloy and SiC_p/2024 Al composite after compensating for the grain-size dependence of plastic flow.

4. Summary

A powder-metallurgy processed 2124 Al alloy was found to be superplastic at high strain rates. A maximum tensile elongation of 700% was achieved at 10^{-2} s^{-1}. The activation energy for the plastic flow measured after the threshold-stress compensation was close to that for lattice diffusion in aluminum. The 2124 Al alloy was revealed to be stronger than the 2124 composite even after the grain-size compensation. When comparing the strength between the unreinforced and reinforced alloys at temperatures where grain boundary sliding dominates the plastic flow, the difference in grain size as well as activation energy for plastic flow and material constant should be taken into account.

Acknowledgement

This work was supported by Hong-ik University fund 1998 and one of authors, Dr. Kim, appreciated for that.

References

1. T. G. NIEH, G. A. HENSHALL and J. WADSWORTH, *Scripta Metall.* **18** (1984) 1045.
2. T. G. NIEH, P. S. GILMAN and J. WADSWORTH, *ibid.* **19** (1985) 1375.
3. T. R. BIELER, T. G. NIEH, J. WADSWORTH and A. K. MUKHERJEE, *ibid.* **22** (1988) 81.
4. T. G. NIEH and J. WADSWORTH, *Mater. Sci. Engr.* **A147** (1991) 129.
5. T. G. NIEH, J. WADSWORTH and T. IMAI, *Scripta Metall.* **26** (1992) 703.
6. M. MABUCHI, K. HIGASHI and T. G. LANGDON, *Acta Metall. Mater.* **42** (1994) 1793.
7. T. R. BIELER and A. K. MUKHERJEE, *Mater. Sci. Engr.* **A128** (1990) 171.
8. K. HIGASHI, T. OKADA, T. MUKAI and S. TAMURA, *Scripta Metall. Mater.* **25** (1991) 2053.
9. T. R. BIELER and A. K. MUKHERJEE, *Mater. Trans. JIM* **32**(12) (1991) 1149.
10. K. HIGASHI, T. OGADA, T. MUKAI, S. TAMURA, T. G. NIEH and J. WADSWORTH, *Scripta Metall.* **26** (1992) 185.
11. M. C. PANDEY, J. WADSWORTH and A. K. MUKHERJEE, *Mater. Sci. Engr.* **80** (1986) 169.

12. G. S. MURTY and M. J. KOCZAK, *ibid.* **100** (1988) 37.
13. DONG-WHA KUM and HAY-SUNG KIM, *Mater. Sci. Forum* **170–172** (1994) 543.
14. W. J. KIM, K. HIGASHI and J. K. KIM, *Mater. Sci. Engr.* **A260** (1999) 170.
15. D. W. KUM, W. J. KIM and G. FROMMEYER, *Scripta Mater.* **40**(2) (1999) 223.
16. T. IMAI, M. MABUCHI, Y. TOZAWA and M. YAMADA, *J. Mater. Sci. Lett.* **9** (1990) 225.
17. M. MABUCHI and K. HIGASHI, *Scripta Mater.* **34**(12) (1996) 1893.
18. Y. LI and T. G. LANGDON, *Acta Mater.* **46**(11) (1998) 3937.
19. R. S. MISHRA, T. R. BIELER and A. K. MUKHERJEE, *Acta Metall. Mater.* **45** (1997) 561.
20. "Metal Handbook Vol; 2, Properties and Selection: Nonferrous Alloys and Pure Metals," 9th ed. (ASM, 1979) p. 78.
21. W. J. KIM, E. TALEFF and O. D. SHERBY, *Scripta Metall.* **32** (1995) 1625.
22. L. KLOC, S. SPIGARELLI, E. CERRI, E. EVANGELISTA and T. G. LANGDON, *Acta Mater.* **45** (1997) 529.
23. K. T. PARK, E. J. LAVERNIA and F. A. MOHAMED, *Acta Metall. Mater.* **42** (1994) 667.
24. Y. LI and T. G. LANGDON, *Acta Mater.* **45** (1997) 4797.
25. A. B. PANDEY, R. S. MISHRA and Y. R. MAHAJAN, *Acta Metall. Mater.* **40** (1992) 2045.
26. O. A. RUANO and O. D. SHERBY, *Mater. Sci. Engr.* **56** (1982) 167.
27. K. T. PARK and F. A. MOHAMED, *Metall. Trans.* **26A** (1995) 3119.
28. W. ZHENG and Z. BAOLIANG, *J. of Mat. Sci. Lett.* **13** (1994) 1806.
29. W. ZHENG, Z. BAOLIANG and W. YANWEN, *Scripta Mater.* **30**(11) (1994) 1367.

Received 30 March
and accepted 22 November 1999